



Published in final edited form as:

*Proc SPIE Int Soc Opt Eng.* 2016 February 27; 9786: . doi:10.1117/12.2216526.

## Random Walk Based Segmentation for the Prostate on 3D Transrectal Ultrasound Images

Ling Ma<sup>a,b</sup>, Rongrong Guo<sup>a</sup>, Zhiqiang Tian<sup>a</sup>, Rajesh Venkataraman<sup>c</sup>, Saradwata Sarkar<sup>c</sup>, Xiabi Liu<sup>b</sup>, Peter T. Nieh<sup>d</sup>, Viraj V. Master<sup>d</sup>, David M. Schuster<sup>a</sup>, and Baowei Fei<sup>\*,a,e,f</sup>

<sup>a</sup>Department of Radiology and Imaging Sciences, Emory University, Atlanta, GA

<sup>b</sup>School of Computer Science, Beijing Institute of Technology, Beijing

<sup>c</sup>Department of R&D, Eigen, Grass Valley, CA

<sup>d</sup>Department of Urology, Emory University School of Medicine, Atlanta, GA

<sup>e</sup>Winship Cancer Institute of Emory University, Atlanta, GA

<sup>f</sup>The Wallace H. Coulter Department of Biomedical Engineering, Georgia Institute of Technology and Emory University, Atlanta, GA

### Abstract

This paper proposes a new semi-automatic segmentation method for the prostate on 3D transrectal ultrasound images (TRUS) by combining the region and classification information. We use a random walk algorithm to express the region information efficiently and flexibly because it can avoid segmentation leakage and shrinking bias. We further use the decision tree as the classifier to distinguish the prostate from the non-prostate tissue because of its fast speed and superior performance, especially for a binary classification problem. Our segmentation algorithm is initialized with the user roughly marking the prostate and non-prostate points on the mid-gland slice which are fitted into an ellipse for obtaining more points. Based on these fitted seed points, we run the random walk algorithm to segment the prostate on the mid-gland slice. The segmented contour and the information from the decision tree classification are combined to determine the initial seed points for the other slices. The random walk algorithm is then used to segment the prostate on the adjacent slice. We propagate the process until all slices are segmented. The segmentation method was tested in 32 3D transrectal ultrasound images. Manual segmentation by a radiologist serves as the gold standard for the validation. The experimental results show that the proposed method achieved a Dice similarity coefficient of  $91.37 \pm 0.05\%$ . The segmentation method can be applied to 3D ultrasound-guided prostate biopsy and other applications.

### Keywords

prostate segmentation; random walk; decision tree; semi-automatic segmentation; 3D transrectal ultrasound image (TRUS)

---

\* bfei@emory.edu; <http://feilab.org>.

## 1. INTRODUCTION

Prostate cancer is one of the major causes of cancer mortality in American men,<sup>1</sup> three-dimensional (3D) transrectal ultrasound (TRUS) can provide 3D visualization of the prostate and relevant anatomical structures. Segmentation of the prostate in 3D-TRUS can have many applications in prostate diagnosis and therapy. Manual segmentation is time-consuming and greatly relies upon the experience of the clinician. Automatic or semiautomatic segmentation can save time and improve the consistency.

Three-dimensional prostate segmentation methods can be divided into four categories: contour based,<sup>2, 3</sup> region based,<sup>4</sup> classification based,<sup>5</sup> and hybrid based methods.<sup>6-9</sup> TRUS images are characterized by low contrast, speckle, micro-calcifications and imaging artifacts. The contour based methods which are dependent on reliable edge information may be adversely affected in the presence of shadow artifacts. Since the prostate is not uniform, the pure region based methods may produce an incomplete prostate region. The intensity heterogeneity and unreliable texture of the prostate gland make it challenging to implement the pure classification based 3D prostate segmentation. A hybrid method can incorporate the different types of algorithms and thus may maximize the advantage of each algorithm and minimize the limitation of each method, therefore it can improve segmentation performance.

In this paper, we introduce a hybrid algorithm combining the region and classification information for 3D segmentation of the prostate. We use a random walk algorithm to express the region information and use the decision tree as the classifier to achieve classification information. Their combination will improve the robustness of the segmentation.

## 2. METHOD

We propose a new semi-automatic segmentation method for the prostate in 3D TRUS images by using a classification based random walk algorithm. Its flowchart is illustrated in Fig. 1. The method includes two stages: the training and segmentation stages. In the training stage, we extract the features for each prostate and non-prostate pixel and train the decision tree. In the segmentation stage, we perform the 3D segmentation by segmenting the prostate slice by slice. For a new patient, based on user interaction, we segment the prostate on the mid-gland slice and obtain a two-dimensional (2D) prostate mask for that slice. We then use that mask, the classification information, and the random walk algorithm to automatically segment the prostate on the adjacent slice until all slices were segmented. The details of the two stages are described below.

### 2.1 The Training Stage

The training stage is to obtain a classifier for guiding the prostate segmentation. It consists of two components: feature extraction and classifier training. Firstly, the features are extracted from each pixel. Then the feature of each pixel and its label (prostate or non-prostate) is used as the training data for training the model of the prostate.

**Feature Extraction**—We choose the adaptive feature description to distinguish between the prostate and non-prostate pixels. We extract the three types of features for each pixel in the ultrasound images.

1. The location information can indicate the possibility of the pixel belonging to the prostate. The location feature is represented by (x, y, z) coordinates of the pixel.
2. The intensity information can reflect the local spatial variation in the boundary. The intensity feature is the intensity value of the pixel.
3. The local binary patterns (LBP) <sup>10</sup> value is a highly discriminative texture descriptor and is insensitive to the gray scale change. The LBP feature is the LBP value encoded by comparing the values between the pixel and its surrounding neighbors.

**Classifier Training**—We train the classifier based on the three features as described above. A decision tree <sup>11</sup> is a tree which consists of a root node, several interior nodes, and leaf nodes. The objective of the decision tree algorithm is to grow the nodes into a tree by splitting the nodes based on the training samples and their labels, where the root node is the entire set of classes while the terminal nodes represent the final classification results. Since a decision tree classifier does not rely on any a priori statistical assumption, we utilize the decision tree algorithm as the classifier to identify the class (prostate or non-prostate) for each pixel.

## 2.2 The Segmentation Stage

**Segmentation of the Mid-Gland Slice**—The random walker algorithm <sup>12</sup> is an interactive segmentation method. It can complete the segmentation by computing the probabilities that unlabeled points first arrive at the seed points which are usually marked by the user. Hence, we initialize our algorithm with the user selecting the apex, mid-gland, and base slices and then marking six foreground (prostate) and background (non-prostate) points on the mid-gland slice. We then fit two ellipses based on these points to obtain more foreground and background points as seed points. Based on these seed points, we run the random walk algorithm to segment the prostate on the mid-gland slice and obtain the segmented mask.

**Segmentation on the Adjacent Slice**—To automatically segment the prostate on the other slices, the important step is to determine the seed points for the random walk algorithm. The user just marks the seed points on the mid-gland slice. For a more accurate location of seed points on the adjacent slice, we use the segmented mask on the last slice and the classification information on the current slice to determine the initial seed points. We assume that the difference between the shape and size of the prostate on the two adjacent images is not likely to be large. Hence, we use the dilation and erosion operations to expand and shrink the mask on the last slice to ensure that the foreground and background points on the last slice are still the foreground and background points on the current slice, respectively. After the dilation and erosion operations, we obtain the possibility of each pixel on the current slice belonging to the foreground and background. On the other hand, according to

the decision tree classifier, we can compute the possibility of each pixel on the current slice belonging to the prostate and non-prostate. By combining them together, we can get the final probability of each pixel in a weighted-sum form. Let  $P_{f1}(i)$  and  $P_{b1}(i)$  be the probability of pixel  $i$  belonging to the foreground and background points according to the mask information, respectively,  $P_{f2}(i)$  and  $P_{b2}(i)$  be the probability according to the classification result, and  $P_f(i)$  and  $P_b(i)$  be the final probability of being the prostate and non-prostate for pixel  $i$ , respectively, and they are computed by

$$\begin{aligned} P_f(i) &= w_1 P_{f1}(i) + w_2 P_{f2}(i), \\ P_b(i) &= w_1 P_{b1}(i) + w_2 P_{b2}(i) \end{aligned} \quad (1)$$

where  $w_1$  and  $w_2$  are the weights assigned to the probability obtained by the segmented mask and classification information, respectively, and they are determined by

$$\begin{aligned} w_1 &= \text{power} \left( \exp(Va), \frac{NofD}{NofAB} \right), \\ w_2 &= 1 - w_1 \end{aligned} \quad (2)$$

The  $NofD$  and  $NofAB$  means the absolute difference between the number of the current slice and the mid-gland slice, and the absolute difference between the number of the apex and base slice, respectively, and parameter  $Va$ , a coefficient to set a tradeoff between the impacts of the two factors, is determined by experiments. If we set  $Va$  to a minus value and  $NofD/NofAB$  must be a positive number of less than 1, we can get a decreasing function. We can say that the value of  $w_1$  is getting smaller with the increment of  $NofD$ , and the value of  $w_2$  is getting bigger, that means the influence of the classification information becomes more important.

Based on the seed points, we run the random walk algorithm for the 2D prostate segmentation and propagate the process from the middle to the base and apex of the prostate until all slices were segmented. Finally, we combine all the 2D prostate masks to form a 3D segmented prostate and use a Gaussian function to smooth the 3D prostate.

### 2.3 Evaluation

The performance of the algorithm is evaluated by Dice similarity coefficient (DSC), Sensitivity (SE), specificity (SP) and false negative rate (FNR). Let S and G be the binary masks from our method and the manual segmentation by a radiologist, respectively.

Dice similarity coefficient (DSC) is the relative volume overlap between S and G. The DSC can be computed as:

$$DSC = \frac{2 \times TP}{(FP + TP) + (TP + FN)}, \quad (3)$$

where  $TP$ ,  $TN$ ,  $FP$ ,  $FN$  is the number of true positives, true negatives, false positives and false negatives, respectively. If a prostate pixel can be classified as a prostate pixel correctly, we call it “true positive”. If a prostate pixel can be classified as a non-prostate incorrectly, we call it “false negative”. In the same way, “true negative” means that a non-prostate pixel can be recognized into non-prostate correctly whereas “false positive” means that a non-prostate pixel is recognized into prostate incorrectly.

Sensitivity (SE) and specificity (SP) are widely used in the medical image analysis, which are essentially two measurements of performance. Sensitivity measures the proportion of prostate pixels which are correctly identified as prostate while specificity measures the proportion of non-prostate pixels which are correctly identified as non-prostate. They are determined by:

$$\begin{aligned} \text{Sensitivity} &= \frac{TP}{TP+FN} \\ \text{Specificity} &= \frac{TN}{TN+FP} \end{aligned} \quad (4)$$

False negative rate (FNR) is an evaluation criterion of error detection. The FNR can be defined as the number of false negative voxels divided by the total number of the prostate voxels on the gold standard. It is computed by

$$FNR = \frac{FN}{TP+FN}. \quad (5)$$

### 3. EXPERIMENT

#### 3.1 Databases

We collected 32 3D transrectal ultrasound image volumes from patients who were clinically selected to undergo the prostate biopsy procedure. An end-firing 5–9 MHz TRUS transducer probe was used for the image acquisition. The voxel size of the image is  $0.19 \times 0.19 \times 0.19$  mm<sup>3</sup>. The size of the images is  $448 \times 448 \times 350$  voxels. The prostate was manually segmented by a radiologist slice by slice. We conducted leave-one-out style cross-validation experiments for the prostate segmentation.

#### 3.2 Parameter Tuning

We first tune the two parameters that were used in our approach by using segmentation experiments. The first parameter is the size of dilation and erosion. We tested 20 integers from 1 to 20 pixels to run the random walk algorithm for the segmentation of prostate. For each tested number, we used the segmented mask processed by dilation and erosion on the last slice to choose the foreground and background seed points, that means  $w_1 = 1$  and  $w_2 = 0$  in Eq. 1, and run the random walk algorithm for the prostate segmentation. The results are shown in Fig. 2. The best number is 4 based on the experimental results. This number was used in all the following experiments.

The second parameter is the parameter  $Va$  in Eq.2, which is a coefficient to set a tradeoff between the impacts of the segmented mask information from the last slice and the classification information obtained from the classifier. We perform our method with ten different  $Va$  from  $-10$  to  $-1$  and record the results (Fig. 3). We choose the value of  $-4$  for  $Va$  because it achieved the best performance.

### 3.3 Experimental Results

**The Segmentation Performance on the Mid-Gland Slice**—We randomly choose one volume and manually mark six prostate and non-prostate points on the mid-gland slice in the coronal image. We then use the twelve points to fit the foreground and background ellipses. Based on the points in the ellipses, we run the random walk algorithm to obtain the boundary of prostate on the mid-gland slice. The process is as shown in Fig. 4, where yellow and green points represent the prostate and non-prostate points, respectively, and the boundary marked in blue are obtained by our method and the smooth boundary marked in red is the gold standard from manual segmentation. The segmented boundaries are close to the ground truth and our method is effective.

**Comparison with the other Methods based on the Random Walk**—In order to demonstrate the performance of our method, we compare it with the two segmented methods, which use the information of the mask on the pre-slice and classification information on the current slice, respectively, to determine the foreground and background seed points for the random walk based segmentation. We can call them  $M\_mask$  and  $M\_classification$  for short. In our experiments, we segmented the prostate for the 32 patients by using  $M\_mask$  method,  $M\_classification$  method and our method. The performance measurements recorded are shown in Table 1, where the numbers are described as mean and standard deviation of 32 prostate image volumes in percentage. From the table, the average DSC from our method is 91.37%, which is better than 74.87% from the  $M\_mask$  and 78.87% from the  $M\_classification$ . Our method had a lower FNR of 8.10% as compared to 31.61% and 39.67% of the other two methods. Our average sensitivity is the highest one. Although our specificity is not the best one, our method still achieved a high specificity of 99.17%. Fig. 5 shows the comparison results. Our method achieves better segmentation performance for most patients than the  $M\_mask$  or  $M\_classification$  method.

## 4. CONCLUSIONS

In this paper, a random walk based segmentation algorithm has been proposed for the prostate on 3D ultrasound images for the first time. After being initialized on the mid-gland slice, this method can automatically segment the prostate on other slices by using the classification based random walk algorithm. The random walk method can avoid not only the discretization errors by formulating the segmentation on a graph but also the segmentation leakage and shrinking bias.

This method is initialized with only six seed points of the prostate and non-prostate on one slice, hence it may significantly reduce the labor as compared to manual segmentation. To overcome the limitation that random walk algorithms may be sensitive to the location of seed points, the proposed method incorporates the classification information obtained by

decision tree classifier to automatically locate more accurately seed points on the other slices for a more accurate segmentation. This semi-automatic segmentation method can be used in 3D ultrasound-guided prostate biopsy and other applications.

## 5. ACKNOWLEDGEMENTS

This research is supported in part by NIH grants (CA176684 and CA156775). LM was partially supported by International Graduate Exchange Program of Beijing Institute of Technology. XL was partially supported by National Natural Science Foundation of China (Grant no. 60973059, 81171407) and the Program for New Century Excellent Talents in Universities of China (Grant no. NCET-10-0044). The work was conducted in the Quantitative BioImaging Laboratory in the Emory Center for Systems Imaging (CSI) of Emory University School of Medicine.

## REFERENCES

- [1]. Siegel RL, Miller KD, Jemal A. Cancer statistics, 2015. *CA: a cancer journal for clinicians*. 2015; 65(1):5–29. [PubMed: 25559415]
- [2]. Qiu W, et al. 3D Prostate TRUS Segmentation Using Globally Optimized Volume-Preserving Prior. *Medical Image Computing and Computer-Assisted Intervention MICCAI*. 2014:796–803. [PubMed: 25333192]
- [3]. Yuan J, et al. Efficient 3D Endfiring TRUS Prostate Segmentation with Globally Optimized Rotational Symmetry. *Computer Vision and Pattern Recognition CVPR*. 2013:2211–2218.
- [4]. Nouranian S, et al. A Multi-Atlas-Based Segmentation Framework for Prostate Brachytherapy. *IEEE Transactions on Medical Imaging*. 2014; 34(4):950–961. [PubMed: 25474806]
- [5]. Yang X, Fei B. 3D Prostate Segmentation of Ultrasound Images Combining Longitudinal Image Registration and Machine Learning. *Proc SPIE*. 2012; 8316 83162o-83162o.
- [6]. Akbari H, Fei B. 3D ultrasound image segmentation using wavelet support vector machines. *Med Phys*. 2012; 39(6):2972–84. [PubMed: 22755682]
- [7]. Yang X, et al. Automatic 3D Segmentation of Ultrasound Images Using Atlas Registration and Statistical Texture Prior. *SPIE Medical Imaging*. 2011:796432–796432.
- [8]. Fei B, et al. A Molecular Image-directed, 3D Ultrasound-guided Biopsy System for the Prostate. *Proc SPIE Int Soc Opt Eng*. 2012:831613–831613. [PubMed: 22708023]
- [9]. Akbari H, et al. 3D Segmentation of Prostate Ultrasound Images Using Wavelet Transform. *Proc SPIE Int Soc Opt Eng*. 2011; 7962 79622K-79622K.
- [10]. Ojala T, Pietikäinen M, Harwood D. A comparative study of texture measures with classification based on featured distributions. *Pattern recognition*. 1996; 29(1):51–59.
- [11]. Safavian SR, Landgrebe D. A survey of decision tree classifier methodology. *IEEE transactions on systems, man, and cybernetics*. 1990; 21(3):660–674.
- [12]. Grady L. Random walks for image segmentation. *IEEE Transactions on Pattern Analysis and Machine Intelligence*. 2006; 28(11):1768–1783. [PubMed: 17063682]

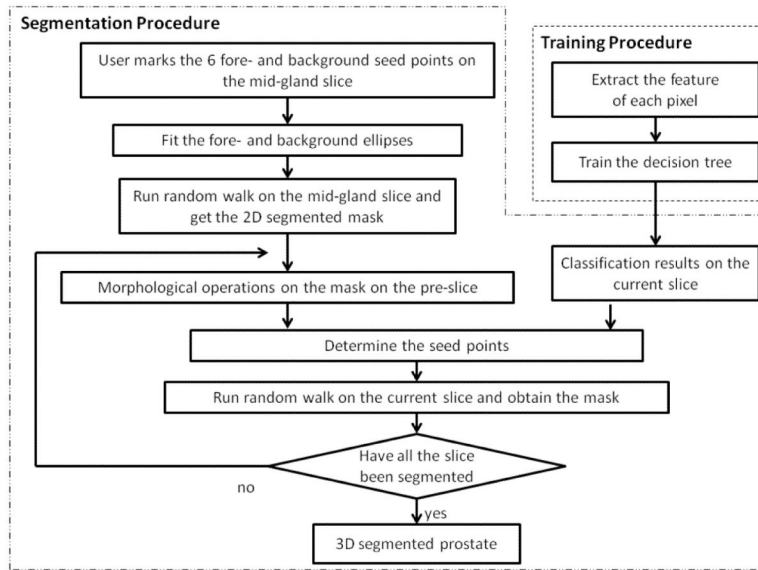


**Figure 1.** Flowchart of the random walk based segmentation.

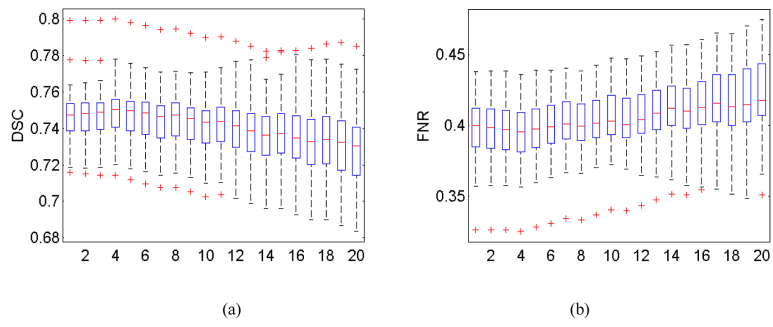


**Figure 2.** The segmentation performance: (a) Dice similarity coefficient (DSC) and (b) False negative rate (FNR) for 32 patients by testing 20 integers from 1 to 20 pixels for the size of dilation and erosion processing.

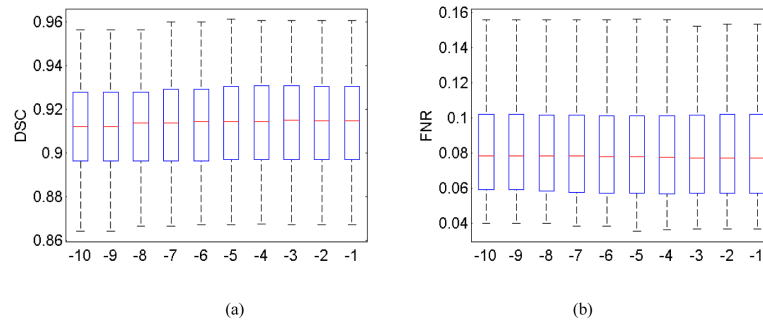


**Figure 3.**  
The segmentation performance (a) Dice similarity coefficient (DSC) and (b) False negative rate (FNR) for 32 patients by testing 10 negative integers from  $-10$  to  $-1$  for the parameter  $V_a$ .

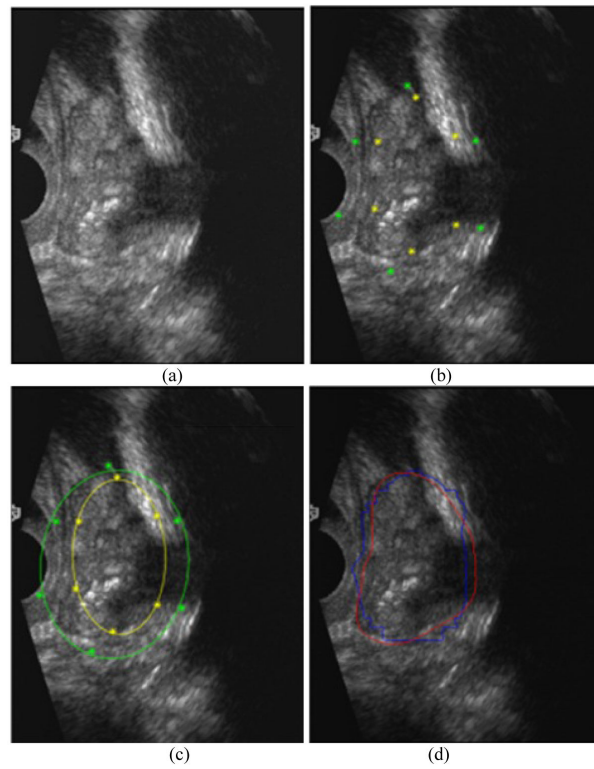


**Figure 4.** Segmentation on the middle slice. (a)-(d) represent the original image, the image with marked points, the image with fitted ellipses, and the image with the segmentation result and the manual segmentation gold standard.

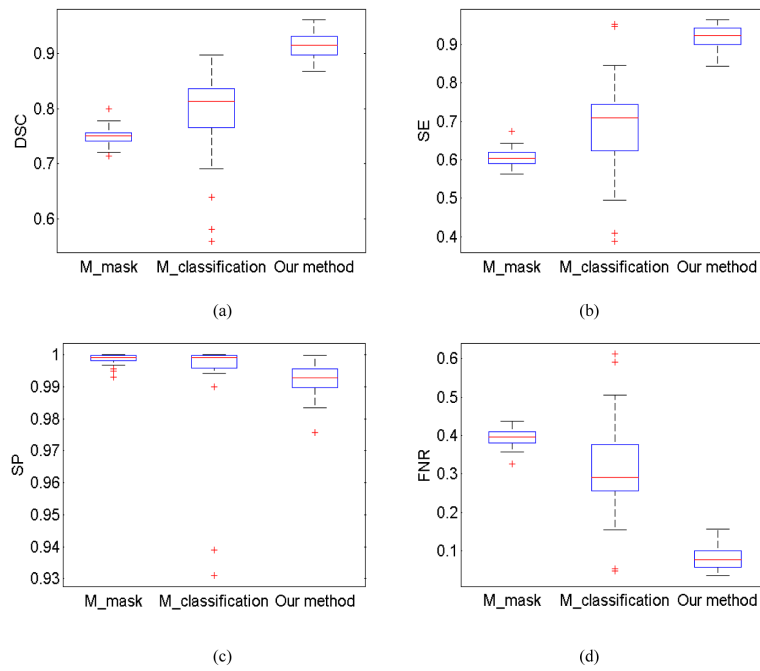


**Figure 5.** The performance of the segmentation. (a) Dice similarity coefficient (DSC), (b) Sensitivity (SE), (c) Specificity (SP) and (d) False negative rate (FNR) for the 32 patient data using the M\_mask method, M\_classification method, and our method.

**Table 1**

The performance of the M\_mask metho, M\_classification method, and our method

	<b>M_mask method</b>	<b>M_classification method</b>	<b>Our method</b>
DSC	74.87±0.03	78.87±0.62	91.37± 0.05
SE	60.33±0.03	68.39±1.58	91.90±0.10
SP	99.87±0.0003	99.41±0.02	99.17±0.002
FNR	39.67±0.05	31.61±1.58	8.10±0.09

Author Manuscript

Author Manuscript

Author Manuscript

Author Manuscript